Available online at www.sciencedirect.com
SCIENCE DIRECT®
Pergamon
Cement and Concrete Research 33 (2003) 1077–1084
CEMENT AND CONCRETE RESEARCH

Heavy metals in cement phases: on the solubility of Mg, Cd, Pb and Ba in $Ca_3Al_2O_6$

A.K. Prodjosantoso[a,b], B.J. Kennedy[a,*]

[a]*The Centre for Heavy Metals Research, School of Chemistry, University of Sydney, Sydney, NSW 2006, Australia*
[b]*Jursan Kimia, Universitas Negeri Yogyakarta, Yogyakarta, DIY 55281, Indonesia*

Received 16 September 2002; accepted 2 January 2003

Abstract

The compounds formed when the divalent cations Mg^{2+}, Cd^{2+}, Ba^{2+} and Pb^{2+} are present during the preparation of $Ca_3Al_2O_6$ have been studied using X-ray microanalysis and diffraction methods. The smaller Mg cations are found to partially substitute for Ca^{2+}, and structural refinements show that Mg preferentially occupies the smaller six-coordinate sites in $Ca_{3-x}Mg_xAl_2O_6$. When Ba is present, it preferentially occupies the larger eight- and nine-coordinate sites. X-ray microanalysis suggests that Pb and Cd are lost from the samples during the preparation process. The diffraction patterns show a small decrease in the lattice parameters, suggesting that a defect structure of the type $Ca_{3-x}(vac)_xAl_2O_6$ is formed. The distribution of products formed on hydration of the doped $Ca_{3-x}M_xAl_2O_6$ is found to be very different than that observed for the undoped material.

Keywords: Heavy metals; Crystal structure; X-ray diffraction; $Ca_3Al_2O_6$

1. Introduction

The is considerable interest in the crystal chemistry of the phases found in cements, driven both by the immense economic importance of cement and by the trend to use alternate starting materials and fuels in the manufacture of cement clinkers [1]. This latter approach can introduce impurity cations into the cement, which in turn can alter the properties of the resulting concrete. Studies of $Ca_3Al_2O_6$, a key component of Portland cement, have shown that the Ca can be partially substituted by a number of other cations, especially Sr [2]. Solid solutions also result when $Ca_3Al_2O_6$ is prepared in the presence of oxides such as Fe_2O_3, Na_2O, K_2O and MgO [3].

Traditionally, only the amount of the "impurity" cation present in the cement has been quantified. Such analyses have shown that Portland cements can contain up to 2 wt.% MgO [4]. However, Portland cement clinkers contain at least four major crystalline phases [1], including $Ca_3Al_2O_6$, and how the Mg is distributed over the four phases is unknown, although there is evidence to suggest that it is not uniformly distributed. Likewise, the fate of other cations, including Ba and the toxic heavy metals Cd and Pb, is unknown although these are known to be able to substitute for Ca in a range of minerals [5]. Similarly, cations such as Cr and Fe partially substitute for Al in minerals [6]. It is probable that the additional cations may be preferentially incorporated into a particular crystalline phase, altering the properties of this phase or significantly altering the relative abundance of this phase in the clinker.

In the present work, we have explored the solubility of Mg, Cd, Pb and Ba in $Ca_3Al_2O_6$ using a combination of electron microscopy, X-ray microanalysis and powder X-ray diffraction methods. In principle, these four cations could all partially replace Ca to form an oxide of the type $Ca_{3-x}M_{x}Al_2O_6$ similar to that described recently for the Sr-substituted series $Ca_{3-x}Sr_xAl_2O_6$ [2]. Since the charge on these cations are that same as that of Ca, it is anticipated that the host framework would be unaltered and that the dopant cations would occupy sites within the rings formed by the six corner-sharing AlO_4 tetrahedra. The reactions of these substituted materials with water are also reported.

* Corresponding author. Tel.: +61-2-9351-2742; fax: +61-2-9351-3329.
E-mail address: b.kennedy@chem.usyd.edu.au (B.J. Kennedy).

0008-8846/03/$ – see front matter.
doi:10.1016/S0008-8846(03)00017-6

2. Experimental

2.1. Sample preparation

The various magnesium, cadmium, lead and barium doped calcium aluminates ($Ca_{3-x}M_xAl_2O_6$, M = Mg, Cd, Pb and Ba) were prepared from mixtures of analytical grade $CaCO_3$ (Merck), $MgCO_3$ (BDH), $BaCO_3$ (BDH), $Cd(NO_3)_2{\cdot}4H_2O$ (Aldrich), $Pb(NO_3)_2$ (Merck) and $Al(NO_3)_3{\cdot}9H_2O$ (Aldrich). For each composition, the appropriate stoichiometric mixture was very thoroughly ground with acetone in an agate mortar and pestle for several minutes. The mixtures were then transferred to alumina crucibles and heated in air successively at 700, 800, 900 and 1000 °C for 24 h each. Finally, the samples were annealed in air at 1100 °C for 72 h or in the case of the Cd- and Pb-doped materials 1200 °C for 24 h, whilst for the Ba-doped materials the final heating step was at 1450 °C for 24 h. For the undoped and lightly Mg-doped samples, crystalline single-phase samples of C_3A[1] were formed on heating at 1100 °C. However, for the Cd-doped samples, noticeable amounts of CdO were present after heating to 1100 °C, whilst the Pb-doped samples were poorly crystalline before heating to 1200 °C. The resulting samples were then characterized using powder X-ray diffraction.

2.2. Sample hydration

Samples were hydrated by adding H_2O in the mole ratio of 100:1. The mixtures were stirred for 1 day under a nitrogen atmosphere at ambient temperature. The reactions were terminated by addition of acetone, and the solids were collected by filtration and then dried under a stream of dry nitrogen.

2.3. Structural measurement and analysis

The powder X-ray diffraction patterns were collected on a Siemens D-5000 diffractometer in 0.02° steps over the angular range $5 < 2\theta < 90°$ using Cu $K\alpha$ radiation. Counting times of up to 15 s per step were employed. The synchrotron X-ray diffraction patterns were collected in 0.01° steps over the angular range $5 < 2\theta < 125°$ on Beamline 20B, the ANBF, at the KEK-Photon Factory Tsukuba, Japan [7] using a wavelength of 0.99859 Å.

Structures were refined by the Rietveld [8] method using the program Rietica [9] operating on a personal computer. The structures of $Ca_{3-x}Mg_xAl_2O_6$, $x = 0.1$, 0.15 and 0.2, were also refined from synchrotron X-ray diffraction data. The structural refinements initially used the structural parameters reported by Mondal and Jeffery [10] for $Ca_3Al_2O_6$. These parameters were also initially used in the structural refinements of Cd- and Pb-doped compounds, whilst the structural parameters reported by Alonso et al. [11] for $Sr_3Al_2O_6$ were employed to generate a starting model for the refinement of the structure of the Ba-doped compound.

In the initial stages of the refinements, it was assumed that all the dopant cations had been incorporated into the crystalline phases and that there was a statistical distribution of Ca and the dopant cations over the six available M^{2+} sites. The positions and atomic displacements of the atoms occupying the same crystallographic site were constrained to be equal. Once the refinements had converged, a number of anomalous atomic displacement parameters were observed and the possibility of either ordering of the Ca and Mg, Pb, Cd or Ba in particular sites or partial loss of the dopant cation was then considered. This ultimately led to an improvement in the various measures of fit and more physically reasonable atomic displacement parameters. The final refinements employed up to 32 positional parameters, 14 isotropic displacement parameters, 4 background parameters and 6 profile parameters.

2.4. Electron microscopy and analysis

Scanning electron micrographs (SEM) were collected using a JEOL JSM6000F or a Philips 505 microscope. Microanalysis was performed with an EDAX PV9900 system.

3. Results and discussion

SEM of the various samples shows the materials to be highly crystalline, although there is no dominant morphology (Fig. 1). X-ray microanalysis (EDA) at numerous points in each sample indicates that the materials are homogenous and there is no evidence for bulk segregation of any elements. Stephan et al. [12] have observed considerable segregation of Cr and Ni when high concentrations of these elements are present during the formation of the clinker, with only a small portion of these dopants being incorporated into the crystalline phases. The average Mg content determined by EDA is slightly higher than the expected stiochiometry at all points studied in the samples, possibly as a result of overlap between the Mg and the Al lines in the EDA spectra (Fig. 2). The measured composition for the only single-phase Ba compound studied is in excellent agreement with the expected values. No Cd or Pb was observed in the appropriate samples (Table 1). While the detection limit of EDA is typically limited to the ppm [13] range, it can be concluded that both these elements evaporated during the preparation of the samples.

The diffraction results (Fig. 3) demonstrate that at low doping levels highly crystalline samples of the type $Ca_{3-x}M_xAl_2O_6$ could be formed by solid state reactions using $Al(NO_3)_3{\cdot}9H_2O$ as a reactive source of Al. The cubic

[1] C_3A is a cement notation for $Ca_3Al_2O_6$, and another short notation $C_{12}A_7$ is $Ca_{12}Al_{14}O_{33}$.

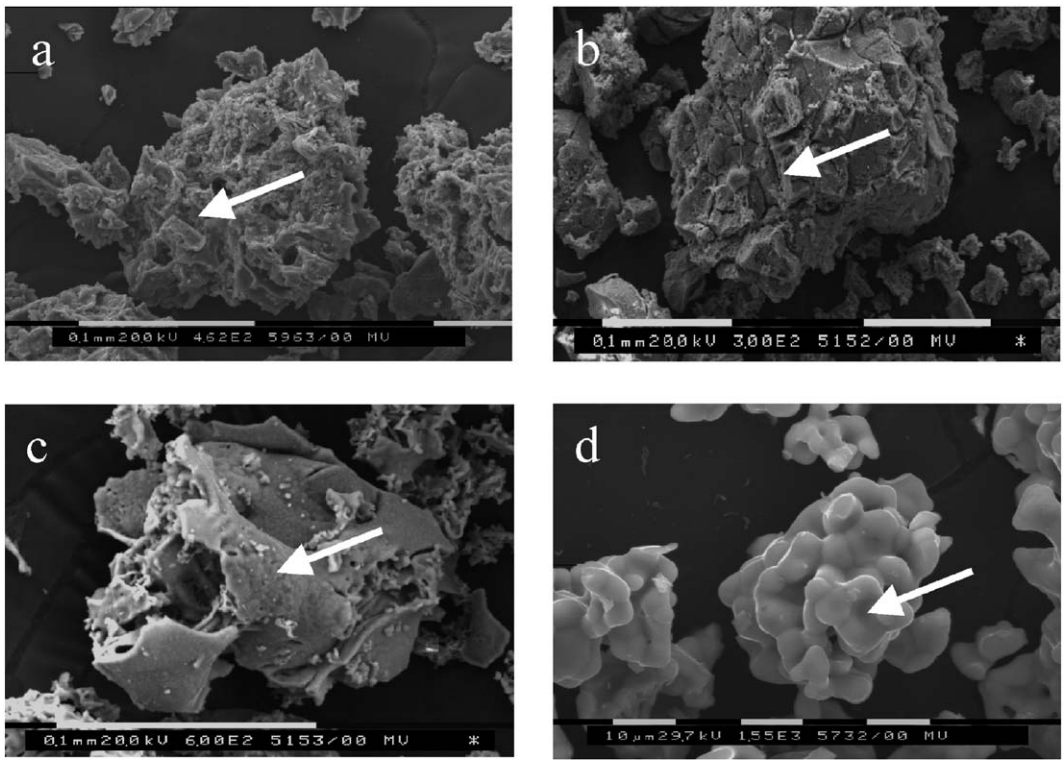

Fig. 1. Representative examples of SEM micrographs for $Ca_{3-x}M_xAl_2O_6$: (a) M=Mg, x=0.15, (b) M=Cd, x=0.1, (c) M=Pb, x=0.1 and (d) M=Ba, x=2.33. The arrows show the areas analyzed using EDA illustrated in Fig. 2.

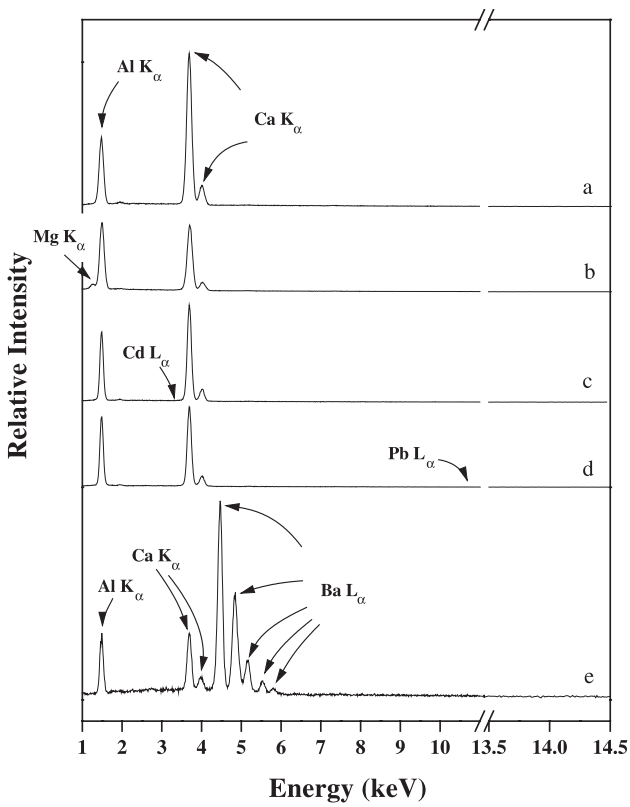

Fig. 2. EDA spectra for $Ca_{3-x}M_xAl_2O_6$: (a) M=Mg, x=0.15, (b) M=Cd, x=0.1, (c) M=Pb, x=0.1 and (d) M=Ba, x=2.33.

$Ca_3Al_2O_3$ structure consists of rings of six corner-sharing AlO_4 tetrahedra with the resulting Al_6O_{18} rings centered on a threefold axis and held together by the Ca/M cations (Fig. 4) [2]. There are six sites occupied by the Ca(M) cations (Table 2). These can be divided into two groups: the three six-coordinate M(1), M(2) and M(3) sites and the three eight- or nine-coordinate sites M(4), M(5) and M(6).

3.1. Mg-doped $Ca_3Al_2O_6$

The powder diffraction patterns for the six compounds in the series $Ca_{3-x}Mg_xAl_2O_6$, x=0, 0.025, 0.05, 0.1, 0.15, 0.2, 0.25 and 0.5, were all very similar (Fig. 3). In all cases, small amounts of a second phase identified as $Ca_{12}Al_{14}O_{33}$ were observed [14]; the amount of this phase increasing as the Mg content was increased. Using a two-phase model in the Rietveld refinements leads to a satisfactory fit to the observed diffraction patterns in all cases (Fig. 5). It appears that Mg may stabilize the $Ca_{12}Al_{14}O_{33}$ over $Ca_3Al_2O_6$. In the x=0.25 and 0.5 samples, additional peaks were observed and these were identified as coming from $MgAl_2O_4$ [15]. Further studies are required to establish if the change in phase abundance is a consequence of incorporation of Mg into $Ca_{12}Al_{12}O_{33}$ or if it is a consequence of the altered Ca/Al ratio. Due to the growth of these competing phases, samples with still higher Mg contents were not investigated. Clearly, under the conditions used to prepare the samples, the solubility of Mg in $Ca_3Al_2O_6$ is limited.

Table 1
Cation ratios for the $Ca_{3-x}M_xAl_2O_6$ samples determined using eda

$Ca_{3-x}M_xAl_2O_6$, x =	Ca	*M*	Al
M = *Mg*			
0.025	3.05	0.05	1.90
0.05	3.04	0.07	1.89
0.1	2.90	0.14	1.96
0.15	2.88	0.17	1.95
0.2	2.75	0.27	1.98
M = *Cd*			
0.01	3.02	0	1.98
0.025	3.02	0	1.98
0.05	3.04	0	1.96
0.1	3.06	0	1.94
M = *Pb*			
0.01	3.04	0	1.96
0.025	3.02	0	1.98
0.05	2.96	0	2.04
0.1	2.95	0	2.05
M = *Ba*			
2.33	0.68	2.35	1.97

The values are estimated to be precise to within ±0.005.

Considering the major phase formed at low Mg levels ($Ca_{3-x}Mg_xAl_2O_6$) than the various Bragg reflections seen in the X-ray diffraction, patterns exhibit a gradual shift in the positions towards higher angles as the amount of the smaller Mg cation present increases, indicating a contraction in the cell size. Pure $Ca_3Al_2O_6$ has a cubic structure (in space group $Pa\bar{3}$ [2]) with $a = 15.2712(6)$ Å and this decreases to 15.2634(5) Å in $Ca_{2.8}Mg_{0.2}Al_2O_6$. The variation in the cell parameters across the series was well reproduced by a simple quadratic of the form $a = 15.27148 - 0.02706x - 0.06084x^2$ where x is the Mg content, as shown in Fig. 6.

Table 2 gives the refined site occupancies for the Mg-doped compounds. For the three doped samples ($x = 0.1$, 0.15 and 0.2), the structural refinements suggested that the Mg preferentially occupies the two six-coordinate (4a and 4b) sites and that no Mg is located within the sites with higher coordination environments. In general, the improvement in the fits of the ordered model over the randomly distributed model was relatively small, presumably as a consequence of the low level of doping and the similarity in the atomic numbers of Mg ($z = 12$) and Ca ($z = 20$). A similar trend was observed when higher-resolution synchrotron diffraction data were used in the structural refinements, these data giving more precise structural parameters. For the two very lightly doped samples ($x = 0.025$ and 0.05), the sites occupied by the Mg could not be unequivocally identified from the structural refinements; however, in all probability, it is located in the six-coordinate sites.

3.2. Ba-doped $Ca_3Al_2O_6$

Although $Ba_3Al_2O_6$ is known to be isostructural with Ca_3Al_2O6 [16], the preparation of samples of the solid solution $Ca_{3-x}Ba_xAl_2O_6$ was not successful under the conditions employed in this work. In general, the products contained appreciable amounts of $BaAl_2O_4$ [17]. A sample of composition $Ca_{0.66}Ba_{2.33}Al_2O_6$ containing only a trace amount of $BaAl_2O_4$ was obtained by heating the reactants at

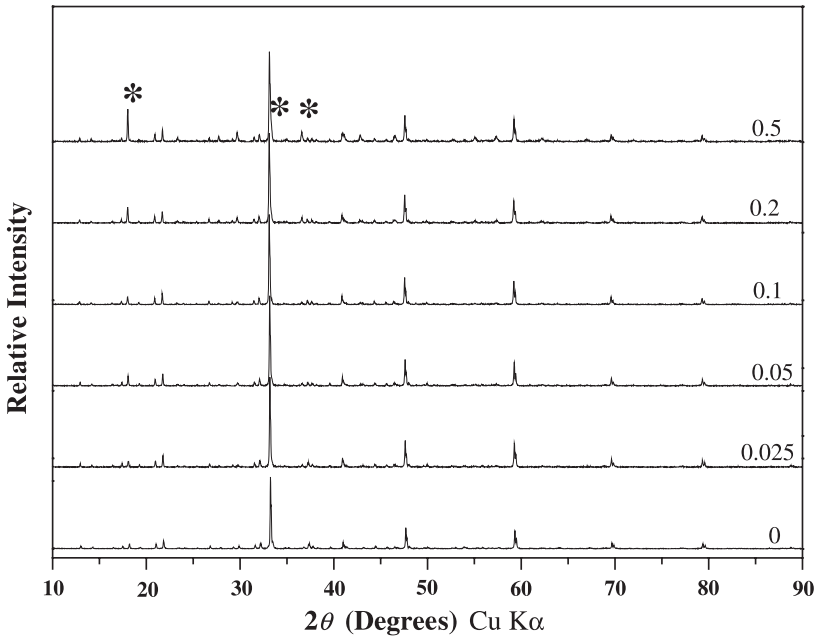

Fig. 3. The powder X-ray diffraction patterns of $Ca_{3-x}Mg_xAl_2O_6$: $x = 0$, 0.025, 0.05, 0.1, 0.15, 0.2, 0.25 and 0.5. The peaks labeled (*) are due to $Ca_{12}Al_{14}O_{33}$. The corresponding *d*-space range is 8.8–1.09 Å.

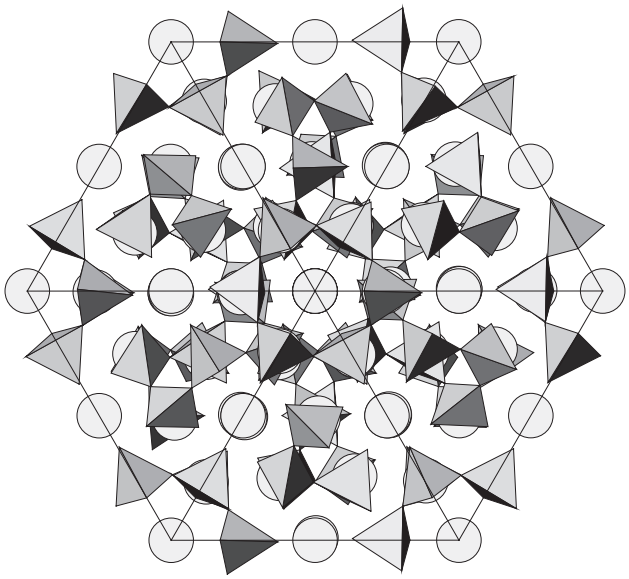

Fig. 4. Representation of the structure of $Ca_3Al_2O_6$. The shaded tetrahedra represent AlO_4 units and the circles represent the various types of divalent (Ca, Mg and Ba) cations.

1450 °C. Refinement of the structure of this sample confirmed it to be isostructural with pure $Ca_3Al_2O_6$; the larger lattice parameter 16.1804(3) Å relative to that of $Ca_3Al_2O_6$ $a = 15.2745(5)$ Å is in accord with the size difference between Ba^{2+} in an eight-coordinate site (IR 1.42 Å) and Ca^{2+} (IR 1.12 Å) [18]. Using a disordered cation model (all six sites having a statistical distribution of Ba and Ca) resulted in an unacceptably poor fit to the observed diffraction data ($R_p = 28.0$, $R_{wp} = 36.4$, $\chi^2 = 5.953$). Allowing for cation ordering resulted in a dramatic improvement in the fit ($R_p = 16.1$, $R_{wp} = 22.7$, $\chi^2 = 2.318$) to the diffraction data. The sensitivity of the refinements to the distribution of the Ca and Ba is a direct consequence of the difference in the atomic number (scattering power) of these two elements. The structural refinement showed that the Ba was located in the eight- or nine-coordinate sites, and none was present in the six-coordinate sites.

3.3. Pb- and Cd-doped $Ca_3Al_2O_6$

As indicated above, the X-ray microanalysis of these samples showed them not to contain the target heavy metals (Cd or Pb). Nevertheless, small differences are apparent between the various diffraction patterns. In particular, the lattice parameters for the four samples prepared using $Cd(NO_3)_2$ as a starting materials show a small reduction in their lattice parameter from that observed for pure $Ca_3Al_2O_6$ (Table 2). The amount of $Ca_{12}Al_{14}O_{33}$ observed in these samples is somewhat higher than that found for the undoped sample, suggesting the change in stiochiometry (lower Ca/Al ratio) favors this. We note that the incorporation of Cd is expected to have little effect on the lattice

Table 2
Selected structural and refinement parameters for $Ca_{3-x}Mg_xAl_2O_6$ obtained from Rietveld analysis of powder X-ray diffraction data

X	a (Å)	Occupancy of M atoms in the site						R_p (%)	R_{wp} (%)	R_{exp} (%)	R_{Bragg} (%)
		M(1) 4a site	M(2) 4b site	M(3) 8c site	M(4) 8c site	M(5) 24d site	M(6) 24d site				
$Ca_{3-x}Mg_xAl_2O_6$											
0	15.2745(5)	–	–	–	–	–	–	15.72	23.01	15.50	6.99
0.025	15.2712(6)	–	–	–	–	–	–	17.49	25.78	13.59	5.72
0.05	15.2694(6)	–	–	–	–	–	–	18.09	27.37	13.12	6.34
0.1	15.2680(5)	0.22(4)	0.18(4)	–	–	–	–	17.88	25.67	18.27	4.88
0.1	15.2552(3)[a]	0.29(2)[a]	0.11(2)[a]	–	–	–	–	6.98[a,b]	7.59[a,b]		
0.15	15.2666(5)	0.33(5)	0.27(5)	–	–	–	–	18.57	27.09	17.26	5.40
0.15	15.2533(3)[a]	0.40(2)[a]	0.20(2)[a]	–	–	–	–	7.40[a,b]	8.08[a,b]		
0.2	15.2634(5)	0.43(5)	0.37(5)	–	–	–	–	17.07	25.88	16.12	5.13
0.2	15.2507(4)[a]	0.52(2)[a]	0.28(2)[a]	–	–	–	–	7.15[a,b]	7.81[a,b]		
$Ca_{3-x}Cd_xAl_2O_6$											
0.01	15.2736(3)	–	–	–	–	–	–	20.87	28.36	12.02	8.04
0.025	15.2731(4)	–	–	–	–	–	–	22.41	32.70	12.81	10.48
0.05	15.2722(5)	–	–	–	–	–	–	16.87	25.73	12.87	6.02
0.1	15.2719(7)	–	–	–	–	–	–	15.08	22.60	12.93	4.43
$Ca_{3-x}Pb_xAl_2O_6$											
0.01	15.2749(3)	–	–	–	0.0004(10)	–	–	22.01	30.64	13.54	11.52
0.025	15.2746(3)	–	–	–	0.003(8)	–	–	11.84	24.53	13.13	6.92
0.05	15.2724(3)	–	–	–	0.003(8)	–	–	16.74	24.52	13.33	6.67
0.1	15.2719(6)	–	–	–	0.004(8)	–	–	14.29	20.77	13.19	4.92
$Ca_{0.66}Ba_{2.33}Al_2O_6$	16.1804(3)	–	–	0.46(6)	1.33(6)	5.2(5)	9.2(5)	15.46	21.78	14.90	6.64

[a] Represents refined results obtained from synchrotron data.
[b] Represents R_p total and R_{wp} total value.

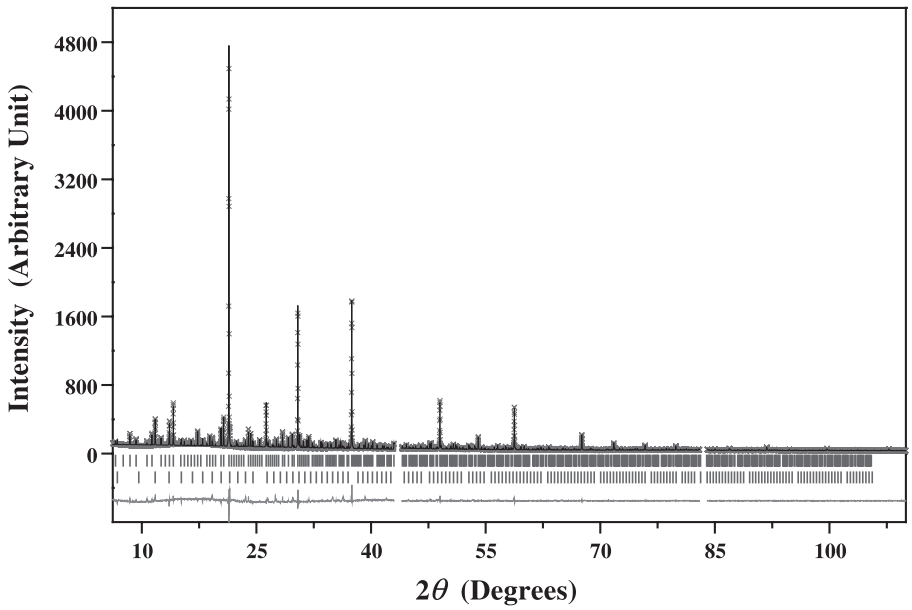

Fig. 5. Observed, calculated and difference diffraction patterns for the synchrotron X-ray diffraction data of $Ca_{2.85}Mg_{0.15}Al_2O_6$. The vertical markers show the positions for all the allowed Bragg reflections. The corresponding *d*-space range is 7.2–0.57 Å.

parameter of $Ca_3Al_2O_6$ since the ionic radii for six-coordinate Cd^{2+} (0.99 Å) is only slightly larger than that for Ca^{2+} (0.95 Å) [18] in the same environment. The refined lattice parameter for the $x=0.1$ Cd sample 15.2719(7) Å is noticeably less than that for pure $Ca_3Al_2O_6$ $a=15.2745(5)$ Å. Likewise, the lattice parameter for the two Pb samples prepared for $x=0.05$ and 0.1 are significantly less than that in pure $Ca_3Al_2O_6$ (Table 2). If Pb was incorporated in these samples, then it would be expected to result in an increase in the cell size since Pb^{2+} (1.18 Å) is larger than Ca^{2+} (0.95 Å) in the same environment [18].

It is possible that the reduction in the lattice parameter observed for both the Cd and the Pb series of compounds is a result of the introduction of vacancies into the lattice; that is, the stiochiometry of the oxides prepared is $Ca_{3-x}(vac)_x Al_2O_6$ where vac is a vacant lattice site. It is notable that the lattice parameters for the pairs of compounds ($x=0.05$ and 0.1) of equal x values prepared by attempting to dope with Pb and Cd are equal, suggesting a similar level of vacancies are present.

3.4. Hydration studies

Powder diffraction patterns of the products formed when the Mg-doped samples were treated with water for 24 h are shown in Fig. 6. These patterns demonstrate that the samples

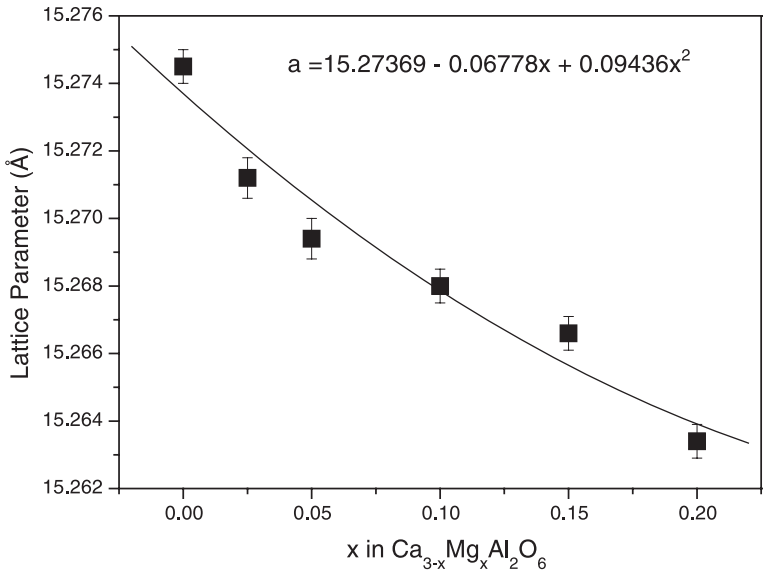

Fig. 6. Composition dependence of the cubic lattice parameter of $Ca_{3-x}Mg_xAl_2O_6$. The solid line is described by the expression shown.

consist of a mixture of at least four phases, namely $CaO{\cdot}Al_2O_3{\cdot}Ca(OH)_2{\cdot}18H_2O$, $Ca_3Al_2O_6{\cdot}xH_2O$, $4CaO{\cdot}Al_2O_3{\cdot}13H_2O$ and $Ca_3Al_2(O_4H_4)_3$. Interestingly, the last of these is the stable hydrogarnet that forms when undoped $Ca_2Al_3O_6$ reacts with water [19] and this is only present at very low levels. As is evident from Fig. 7, the inclusion of only 0.1 mole of Mg to $Ca_3Al_2O_6$ has a dramatic effect on the distribution of the resulting products. More detailed studies of more lightly doped samples are in progress. It is possible that the other three phases seen in the Mg-doped samples would react further on standing to yield the stable hydrogarnet. No crystalline Mg containing compounds were identified in any of the patterns. A mixture of products was also formed on hydration of $Ca_{0.66}Ba_{2.33}Al_2O_6$. Examination of the diffraction patterns shows at least three crystalline phases were present, namely $Ba(OH)_2{\cdot}H_2O$, $Ba(OH)_2{\cdot}3H_2O$ and $Ca_3Al_2(O_4H_4)_3$. The segregation of the Ba and Ca into two different crystalline species is consistent with previous studies on the analogous Sr-doped compounds $Ca_{3-x}Sr_xAl_2O_6$ [19] Hydration of the various $Ca_{3-x}(vac)_xAl_2O_6$ samples, formed when Pb or Cd were included as starting materials, showed the major product to be the stable hydrogarnet, $Ca_3Al_2(O_4H_4)_3$, together with variable amounts of $Ca_3Al_2O_6{\cdot}xH_2O$ and $4CaO{\cdot}Al_2O_3{\cdot}13H_2O$.

4. Conclusions

The potential addition of divalent cations Mg^{2+}, Cd^{2+}, Ba^{2+} and Pb^{2+} to $Ca_3Al_2O_6$ has been studied using X-ray analysis and diffraction methods. When substitution occurs, the size of the divalent cation relevant to that of Ca^{2+} influences the site of substitution. The smaller Mg cations are found to partially substitute for Ca^{2+} and the structural refinements show that Mg preferentially occupies the smaller six-coordinate sites in $Ca_{3-x}Mg_xAl_2O_6$. It was not possible to introduce Ba into $Ba_3Al_2O_6$ unless the firing temperature was increased from 1100 to 1450 °C. When Ba is present, it preferentially occupies the larger eight- and nine-coordinate sites.

X-ray microanalysis suggest that Pb and Cd are lost from the system during the heating process. Nevertheless,

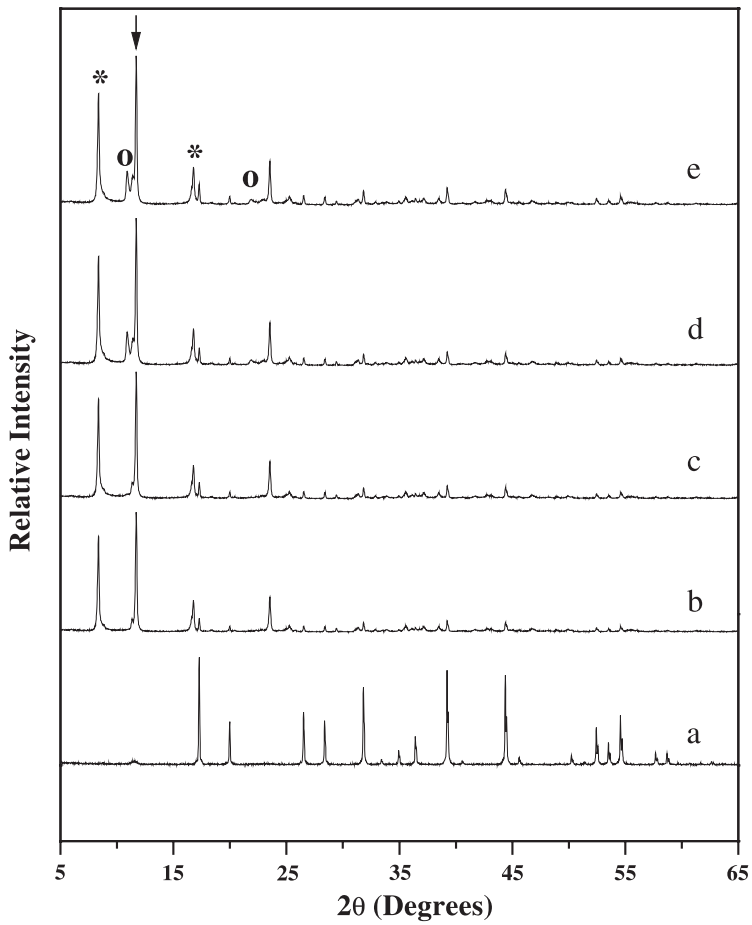

Fig. 7. Powder X-ray diffraction patterns of hydrated $Ca_{3-x}Mg_xAl_2O_6$ where $x = 0$ (a), 0.1 (b), 0.15 (c), 0.2 (d) and 0.25 (e). The symbols show the positions of the strongest reflections due to $CaO{\cdot}Al_2O_3{\cdot}Ca(OH)_2{\cdot}18H_2O$ (*), $Ca_3Al_2O_6{\cdot}xH_2O$ (↓) and $4CaO{\cdot}Al_2O_3{\cdot}13H_2O$ (°). The remaining strong reflections are due to the hydrogarnet $Ca_3Al_2(O_4H_4)_3$. The corresponding *d*-space range is 17.7–1.43 Å.

the diffraction patterns show a small decrease in the lattice parameters, suggesting that a defect structure of the type $Ca_{3-x}(vac)_xAl_2O_6$ is formed. A large amount of $Ca_{12}Al_{14}O_{33}$ is also formed in these samples.

Hydration of the various samples produced a mixture of products. The formation of the otherwise stable hydrogarnet was inhibited by the incorporation of either Mg or vacancies into $Ca_{3-x}M_xAl_2O_6$. This observation, together with the change in the variety of phases formed upon inclusion of the foreign metal, demonstrates the sensitivity of cement to the presence of foreign cations. This is clearly an area deserving of further studies.

Acknowledgements

The synchrotron measurements at the Australian National Beamline Facility were supported by the Australian Synchrotron Research Program, which is funded by the Commonwealth of Australia under the Major National Research Facilities program. We thank Dr. James Hester for his assistance with these measurements.

References

[1] J.C. Taylor, I. Hinczak, C.E. Matulis, Rietveld full-profile quantification of Portland cement clinker: The importance of including a full crystallography of the major phase polymorphs, Powder Diffr. 15 (2000) 7–18.

[2] A.K. Prodjosantoso, B.J. Kennedy, B.A. Hunter, Synthesis and structural studies of strontium-substituted tricalcium aluminate $Ca_{3-x}Sr_xAl_2O_6$, Aust. J. Chem. 53 (2000) 195–202.

[3] Y. Benarchid, A. Diouri, A. Boukhari, J. Aride, R. Castanet, J. Rogez, Thermal study of chromium–phosphorus-doped tricalcium aluminate, Cem. Concr. Res. 31 (2001) 449–454.

[4] H.F.W. Taylor, Cement Chemistry, Academic Press, New York, 1990.

[5] J.-Y. Kim, R.R. Fenton, B.A. Hunter, B.J. Kennedy, Powder diffraction study of synthetic lead and calcium apatites, Aust. J. Chem. 53 (2000) 679–686.

[6] R.M. Cornell, U. Schwertmann, The Iron Oxides, VCH, Weinheim, 1999.

[7] T.M. Sabine, B.J. Kennedy, R.F. Garrett, G.J. Foran, D.J. Cookson, The performance of the Australian powder diffractometer at the photon factory, Japan, J. Appl. Crystallogr. 28 (1995) 513–517.

[8] H.M. Rietveld, A profile refinement method for nuclear and magnetic structures, J. Appl. Crystallogr. 2 (1969) 65–71.

[9] B.A. Hunter, C.J. Howard, A Computer Program for the Rietveld Analysis of X-ray and Neutron Powder Diffraction Patterns, ANSTO, Sydney, 1996.

[10] P. Mondal, J.W. Jeffery, The crystal structure of tricalcium aluminate, $Ca_3Al_2O_6$, Acta Crystallogr., B 31 (1975) 689–697.

[11] J.A. Alonso, I. Rasines, J.L. Srubeyroux, Tristrontium dialuminum hexaoxide: An intricate superstructure of perovskite, Inorg. Chem. 29 (1990) 4768.

[12] D. Stephan, R. Mallmann, D. Knofel, R. Hardtl, High intakes of Cr, Ni and Zn in Clinker: Part 1. Influence on burning process and formation of phases, Cem. Concr. Res. 29 (1999) 1949–1957.

[13] I.M. Watt, The Principles and Practice of Electron Microscopy, 2nd ed., Cambridge Univ. Press, Cambridge, 1997.

[14] A.N. Christensen, Neutron powder diffraction profile refinement studies on $Ca_{11.3}Al_{14}O_{32.3}$ and $CaClO(D_{0.88}H_{0.12})$, Acta Chem. Scand., A 41 (1987) 110–112.

[15] H. Sawada, An electron density residual study of magnesium aluminum oxide spinel, Mater. Res. Bull. 30 (1995) 341–345.

[16] L. Walz, M. Heinau, B. Nickjcurda, Die Kristallstrukturen der Erdalkalialuminate $Ba_3Al_2O_6$ und $Ba_{2.33}Ca_{0.67}Al_2O_6$, J. Alloys Compd. 216 (1994) 105–112.

[17] W. Hörkner, H. Müller-Buschbaum, Zur Kristallstruktur von $BaAl_2O_4$ Z, Anorg. Allg. Chem. 451 (1979) 40–45.

[18] R.D. Shannon, Revised effective ionic radii and systematic studies of interatomic distances in halides and chalcogenides, Acta Crystallogr., A 32 (1976) 751–767.

[19] A.K. Prodjosantoso, B.J. Kennedy, B.A. Hunter, Phase separation induced by hydration of the mixed Ca/Sr aluminates $Ca_{3-x}Sr_xAl_2O_6$: a crystallographic study, Cem. Concr. Res. 32 (2002) 647–655.